EVALUATION OF THE NAWC/AD F/A-18 C/D SIMULATION INCLUDING DATABASE COVERAGE AND DYNAMIC DATA IMPLEMENTATION TECHNIQUES

Cornelius J. O'Connor*, John N. Ralston†
Bihrle Applied Research, Incorporated
18 Research Drive, Hampton, Virginia 23666
Timothy Fitzgerald‡
NAWC/AD - Manned Flight Simulator

ABSTRACT

The NAWC/AD F-18C/D simulation is capable of modeling in-control and out-of-control flight motions in a very representative manner. While many sources of static and dynamic data were considered during analysis of flight motions versus simulation response, the method of implementing dynamic terms was never rigorously examined. This report examines methods of combining dynamic data (steady wind axis rotary and body axis forced oscillation). The current model's static and dynamic data coverage of the angular and rate excursions experienced during out-of-control motions was evaluated. This revealed that extending static sideslip effects to higher sideslip benefits modeling of some out-of-control maneuvers. When implemented using methodology proposed by Kalviste, properly collected dynamic data are capable of providing adequate dynamic definition. When the simulation was revised to incorporate an entirely **as-tested** dynamic data set with the Kalviste mechanization, rigorous correlation with flight test revealed a significant improvement in modeling of flight motions over the original model, which used empirically adjusted forced oscillation terms. Further analysis revealed that much of the improvement results from inclusion of the rotary damping terms and that questions persist regarding body axis testing technique and data.

NOMENCLATURE

The units for physical quantities used herein are presented in U.S. Customary Units, unless otherwise noted.

b	Wing span, ft.
C_l	Rolling-moment coeff., Rolling moment/qsb
C_{lp}	Rolling moment due to roll rate
C_{lr}	Rolling moment due to yaw rate
$C_{l\beta}$	Rolling moment due to sideslip rate
C_n	Yawing-moment coeff., Yawing moment/qsb
C_{np}	Yawing-moment due to roll rate
C_{nr}	Yawing-moment due to yaw rate
$C_{n\beta}$	Yawing-moment due to sideslip rate
q	Free-stream dynamic pressure, lb/ft2
p	Roll rate
Ome	Kalviste technique rotation vector allocation
r	Yaw rate
V	Free-stream velocity, ft/sec
V_T	Velocity vector
α	Angle of attack, deg
β	Angle of sideslip, deg
Ω	Rotation vector
$\Omega b/2V$	Spin coeff., positive for clockwise spin
ω	Angular velocity about spin axis, deg/sec

Subscripts:

Basic	Coeff. effects obtained from basic airframe
Body	Body axis
Dir	Direct technique
Dyn	Total of body and wind axis dynamic term
Filt	Filter technique
Mod	Oscillatory residual (applied to the forced oscillation term) from the Kalviste technique
Osc	Oscillatory residual (applied to the forced oscillation term) from direct or filter technique
Tot	Total coefficient
Wind	Wind axis

INTRODUCTION AND BACKGROUND

The predictive capabilities of the NAWC/AD F-18C/D simulation have been the subject of several database upgrades over the past several years[1, 4-8] with commensurate improvements in the predictive capabilities for the basic airplane, as well as several other loadings. While these improvements have come primarily through the improvement in the definition of the basic airplane static data set, the dynamic characteristics have been adjusted considerably as the database has evolved from the original McDonnell Douglas mechanization to its current form. While the static data changes were generally undertaken to improve the correlation of the model with some known wind tunnel data set, the dynamic data changes, particularly the forced oscillation data, was the subject of "non-rigorous", somewhat empirical, evolution. Some of the changes were the result of how the dynamic data sets (forced oscillation and wind axis rotary data) were combined in the simulation. The work

---

* Senior engineer, member AIAA
† Engineering manager
‡ Engineer, member AIAA

documented in the following report was an attempt to use the existing, high fidelity NAWC/AD simulation as a starting point for the evaluation of how to integrate the diverse data sets available to provide the best possible representation of the airplane behavior, particularly for very dynamic, large angle motions such as spins, departures and large amplitude coupled pitch oscillations (i.e., falling leaf). One of the primary goals was to evaluate potential implementation methods that would minimize the post wind tunnel test manipulation of the simulation data set. The results of this study were a necessary precursor to additional work that would permit a detailed analysis of the predominant forcing functions that cause the F-18 to experience motions such as the falling leaf.

The methods of implementing dynamic test data in the analysis of vehicle motions have been the subject of many studies[9-12] over the years. A number of these efforts have investigated less traditional modeling of an airplane's dynamic characteristics in order to attempt to capture some of the very non-linear and, in some cases time dependent, responses of the airplane. Unfortunately, validation of any of these methods has been sporadic and non-rigorous, consequently, an industry-wide consensus on how the data sets are used to represent the vehicle is not available. Many past and current analyses[13,14] have addressed the complexity of obtaining, analyzing and modeling a vehicle's large amplitude motion. A wide range of concerns arise in the data acquisition process, such as support interference on the dynamic flow field around the model, facility induced effects, Reynolds number effects, etc. These concerns must be reconciled with the ultimate goal of the testing, i.e., the development of a simulation that will aid in the design of a configuration and its flight control system. A modeling philosophy that attempts to identify the strengths and weaknesses of the various data sets used, and augments or accounts for these weaknesses as part of the math model development **can** provide a viable data set for the simulation of these large angle motions. By recognizing the importance of the static data set, and ensuring all the requisite functionality (i.e., sideslip effects on both the basic airplane as well as controls, control interactions, effect of asymmetries, etc.) and non-linearities are adequately modeled, only then can assessment of the second order effects, i.e., the dynamic damping terms, be accomplished.

The integration of these terms into the simulation has been approached in a number of ways. The most common has been to model the dynamic damping based on a linearized body axis damping term, and takes the form of the Taylor series second order rate damping shown in the example below:

$$DCl_{dyn} = Cl_p * p_{body} * b/2V + Cl_r * r_{body} * b/2V \quad (1)$$

The application of this model form has evolved from a period where the description of the airplane dynamic response below stall was most important, but ignores limitations in the strict application of forced oscillation test data as angle of attack approaches and exceeds stall. The most obvious limitation is the assumption that the effect of the wind axis rate terms (i.e., β, etc.) are negligible when the linearized rate terms are expanded by multiplying by a pure body rate. This problem is compounded when the roll and yaw rate terms are additively superimposed to define the damping in a coordinated motion. The assumption that the addition of individually excited linear rate terms will combine to define the damping of a motion that excites both axes simultaneously (with little or no β dot excitation) becomes highly suspect in the stall region. Evidence of this is shown in the flight test correlation[15] and is presented in Figure 1, wherein poor correlation between the flight extracted damping term and the forced oscillation data is exhibited in the stall region for

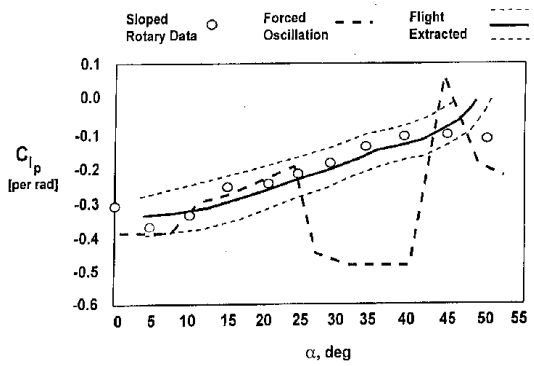

Figure 1. Correlation of Clp

the F/A-18. In this case, the flight derived terms were extracted using the conventional dynamic buildup as described above, and because the maneuvers examined were attempting to maintain a coordinated velocity vector roll rate, β dot was generally not excited. Consequently, the rate terms extracted from flight were the pure rate terms, rather than the composite that results from the forced oscillation data. As shown in Figure 1, the resulting terms actually correlated better with the sloped rotary balance terms than the oscillatory data, as would be expected since the test motion and the flight motion coincide.

Because of these concerns, other schemes of employing both the rotary balance dynamic data along with the body axis forced oscillation data have been developed. As described earlier, several techniques

have been forwarded that employ non-standard data buildup, and while these methods may have validity in modeling large angle motions, they are not used extensively in industry and consequently will not be examined here.

The three methods that have been used in most of the recent attempts to utilize the rotary and forced oscillation data sets are presented in table 1.

DESCRIPTION	COMPONENTS
Direct	
Resolution of rotation rate on velocity vector Ω = pwind pwind = p*cosαcosβ + q*sinβ + r*sinαcosβ	p_{osc} = p - Ωcosβcosα q_{osc} = q - Ωsinβ r_{osc} = r - Ωcosβsinα
Filtered	
Resolution of rotation rate on velocity vector Ω = 1/(τs+1) pwind pwind = p*cosαcosβ + q*sinβ + r*sinαcosβ	p_{osc} = p - Ωcosβcosα q_{osc} = q - Ωsinβ r_{osc} = r - Ωcosβsinα
Kalviste	
Resolution of rotation rate into two components (either p and Ω or r and Ω) based on relative position of velocity vector and rotation vector	p_{mod} = p - Ωcosα q_{mod} = q r_{mod} = r - Ωsinα

Table 1. Examples of dynamic data implementation

The direct resolution of the body axis rates onto the wind axis has been used in recent simulation applications[16]. In an attempt to make the application more representative of the actual test conditions in rotary testing; i.e., "steady wind-axis rotation", a proposed method[9] utilizes a filtered wind axis roll rate as the rotary term ω. This is the implementation scheme currently used in the NAWC/AD F/A-18 simulation. Both this method and the direct resolution technique resolve residual body axis terms that are applied to the forced oscillation data as shown in the table. A third method of resolving the motions was proposed by Kalviste[2] that distributes the aerodynamic damping effects based on the relation of the airplane motion to the actual wind-tunnel test motions used to derive the various damping terms. This is determined by examining the relative position of the velocity vector (V_T) and the rotation vector (Ω). In the simplest terms, when the two vectors are aligned, i.e., in a coordinated rolling maneuver, the damping terms utilized would come from the rotary balance test data since the test motion is a velocity vector roll. When the rotation vector lies on either the x or z body-axes, the dynamic damping would be derived from either the roll or yaw rate derivative respectively, again, because these motions are replicated by the test technique. For conditions where the rotation vector lies between these axes and the velocity vector, the dynamic damping is allocated by resolving the rotation vector (Ω) between the velocity vector (V_T) and the adjacent body axis. This two component resolution assures that the resulting body axis component (designated p_{mod} or r_{mod}) is always a fraction of the total body axis p and r, as opposed to three component resolution where the resolved body axis terms (i.e., p_{osc} or r_{osc}) are frequently the opposite sign of the total rate. In the simulation, the p_{mod} and r_{mod} terms are applied to the body-axis damping derivatives in the conventional expansion (i.e., $p_{mod} * b/2V * C_{lp} = \Delta C_l$) to form the incremental moment effect.

Obviously, the method of dynamic data implementation influences the values of the rates used to apply the various dynamic damping terms, and consequently the predictive capabilities of the simulation itself. The present NAWC/AD F-18C/D simulation uses the older filter technique for the implementation of the dynamic terms, and as discussed earlier, the dynamic terms have evolved as attempts have been made to improve model response using this mechanization scheme. An examination of the data set used, and how these mechanization schemes interact with the results was the major goal of this study.

DISCUSSION OF RESULTS

The task of evaluating the mechanization techniques against the existing database was structured to accomplish several purposes. These goals included the following:

a) Evaluate the coverage, in both the static and dynamic data sets, of the database versus the available flight test data for a wide range of flight conditions.

b) Evaluate the impact of dynamic data mechanization schemes on the resulting simulation response, particularly when compared against flight.

c) These results, as well as any recommendations, formed the basis for an extensive parametric evaluation of the forcing aerodynamic behavior of the F-18's coupled pitch trim, or falling leaf which was evaluated in a subsequent effort[19-21].

Description Of Task

The overall effort can be broken into several distinct portions. The first step was to assemble a body of flight test time history data for appropriate maneuvers in the high-angle-of-attack flight regime.

The primary sources of data used for this effort were from the Controls Released Departure Recovery Test and the Simulation Verification and Validation flights at NAWC/AD, and the HARV flight test program at NASA Dryden. The extracted flight rates and moments of inertia were used to calculate the rolling, yawing, and pitching moment coefficients. The moments of inertia were assumed constant for the calculations since the maneuvers were relatively short in duration.

The flight test time histories were then analyzed to determine the type and range of motions the aircraft actually experiences during these maneuvers. This phase of the analysis included the examination of all first and second order state terms that were excited within the range of flight test motions available, and considerations as to whether these terms were being adequately modeled in the database. This included examination of terms that were not currently modeled, and some evaluation as to their ultimate significance on the predicted motion. This information was used to examine the envelope coverage in the up-and-away portion of the NAWC/AD Phase II F/A-18 database. For example, one shortcoming which became immediately obvious was that during departures the F/A-18 can exceed the 30° sideslip angle limit of the current database. The impact of this type of shortcoming on the ability of the simulation to model these motions was also evaluated.

To determine what areas of the database needed attention, the relative importance of the static and dynamic terms was evaluated. This was done by first "overdriving" the simulation with the rates, attitude, control deflections, and other pertinent parameters from the flight time histories, see figure 2. Overdrive allows the validation of simulation aerodynamic data base against flight-extracted data. At each time slice, extraction of aerodynamic moment coefficient from flight-recorded time history occurs as shown on the right side of figure 2. Angular rates are numerically differentiated to obtain the angular acceleration of the vehicle. After the removal of the inertial effects, the remainder is non-dimensionalized to calculate the aerodynamic force and moment coefficients experienced during flight. Also at each time step, flight-recorded states such as angle of attack, angle of sideslip, control surface positions, etc., are used to exercise the aerodynamic model. Each aerodynamic model element (i.e., pitching moment due elevator, pitching moment due to flap, etc.) is stored and summed as prescribed by the simulation equations. By overplotting the model predicted coefficients with the flight-extracted total coefficients, differences can be easily identified. Correlating the discrepancies with the excitation of individual elements and parameters from the flight time history will help the user to isolate potential weaknesses in the aerodynamic model. It should be emphasized that there is no integration during an overdrive run. The states are completely restricted to the data in the time history, with the advantage that there no propagation of error over time. Any differences between the model-predicted and the

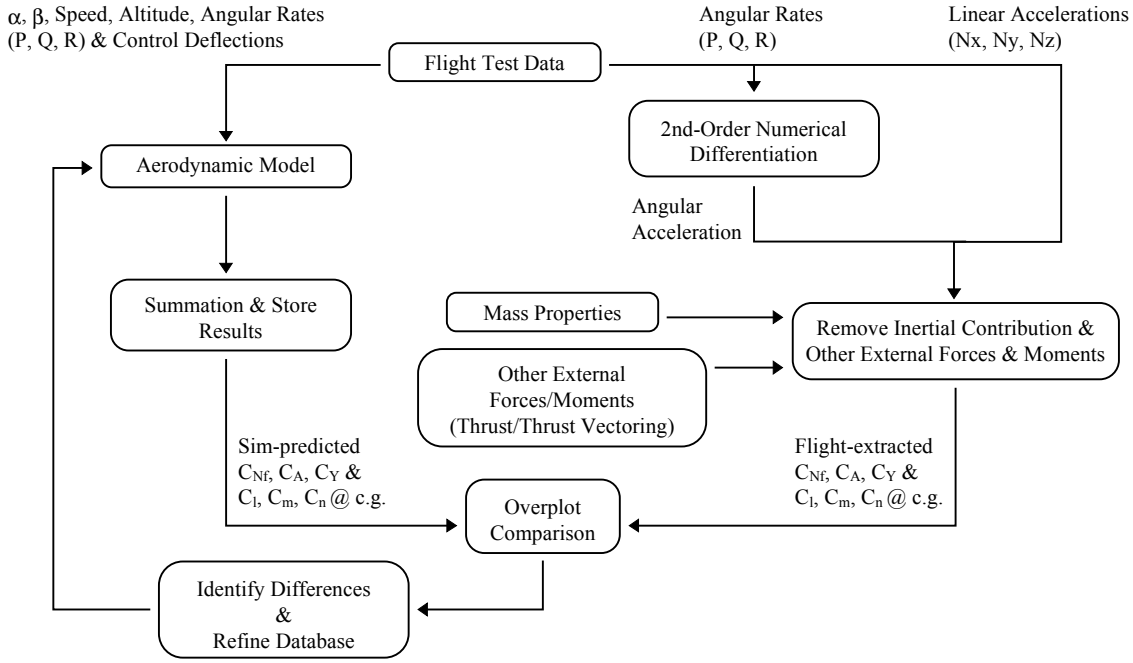

Figure 2. Schematic of 'Overdrive' technique

flight-extracted values are strictly the result of local error. Additionally, the flight control system is by-passed in this methodology thus avoiding any confusion between error caused by aerodynamic modeling and error from the flight control system model. Once the user is satisfied with aerodynamic model, the entire simulation can be validated by running the simulation open-loop, or controlled by flight-recorded pilot input.

As discussed in the introduction, a major focus of this task was to determine the most accurate method of mechanizing the dynamic derivative and rotary balance data in the simulation. Four different mechanization schemes were examined: These included the direct Pwind method, the filtered Pwind method, the Kalviste method, and the classic Taylor series expansion that uses no rotary balance data. Simulation time histories were run for the various flight maneuvers using each of these implementations, and the results were compared to the flight test extracted coefficient data as discussed above.

Evaluation Of Airplane Motions

The evaluation of the database coverage against the available flight data required collecting a range of test data that encompassed both in-control as well as out-of-control flight. A large number of flights were collected and examined. In order to limit the discussion to a manageable level, the following analysis will focus on these significant flight conditions:

1. HARV flight 172.11, a velocity vector roll at 45° angle of attack. (figures 3 and 7).
2. PAX flight 11, a 30° angle of attack departure and recovery (figures 4 and 8).
3. PAX flight 12.9, a low angle of attack departure into a falling leaf (figures 5 and 9).
4. HARV flight 180.4, an intermediate spin (figure 6).

In-Control Motions

Typical aircraft motions during the majority of up and away flight consist of various combinations of coordinated rolling maneuvers and pitching maneuvers. Intentional sideslipping and generation of pure body axis lateral directional rates were rarely encountered during examination of most of the available flight test database, particularly as angle of attack is increased. With the exception of very low angles of attack, the F-18 C/D flight control system attempts to coordinate both lateral stick and rudder inputs to minimize sideslip buildup. As a result, most maneuvering flight test data revealed that when resolved to the wind axis, using either the direct or Kalviste method, there was little residual body axis roll or yaw rate terms. This is

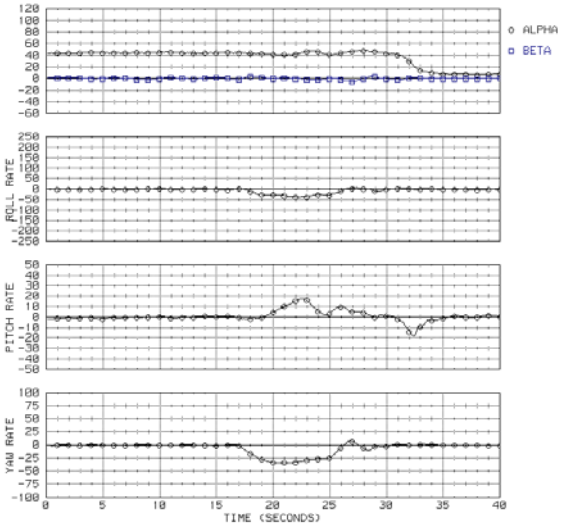

Figure 3a. Velocity vector roll rates and angles

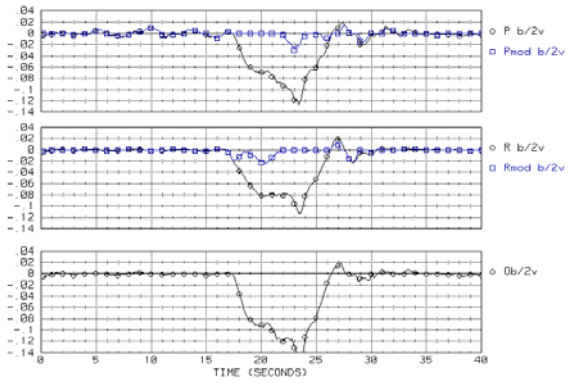

Figure 3b. Velocity vector roll non-dimensional rates

illustrated in figure 3b for the 45° angle of attack coordinated roll maneuver.

Because these maneuvers are coordinated at a fixed angle of attack, little α dot or β dot excitation occurs. As discussed earlier, the wind axis rotational damping (rotary balance) data provides a very representative data set for describing the dynamic behavior in these types of motions. Also shown by these results, the range of non-dimensional rates excited extends beyond 0.1 (well beyond the typical forced oscillation test range of less than 0.01), depending on how the data is resolved. Because of known non-linear behavior on rotary damping terms in the stall / post stall region[4], the non-linear characterization of any body axis damping terms would seem to be required.

Departure / Out of Control Motions

For the F-18, departures are typically characterized by large sideslip excursions, high non-

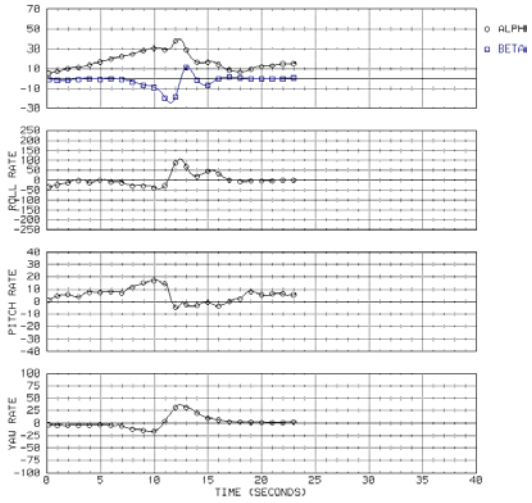

Figure 4a. Departure at 30° aoa, rates and angles

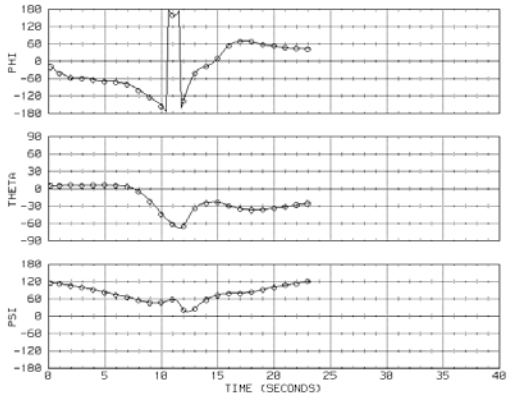

Figure 4b. Departure at 30° aoa, angles

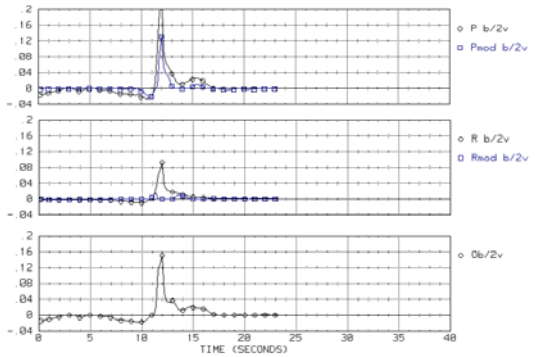

Figure 4c. Departure at 30° aoa, non-dimensional rates

dimensional body axis rate build up, followed by moderate to high angle of attack excursions depending on the severity of the departure. A mild departure is depictedin figures 4 and 8. The departure results following a roll reversal of a slow down turn up to 30° angle of attack with the two seat center line tank equipped configuration. During the roll reversal, adverse sideslip angle builds until the lateral stability abruptly reverses the roll rate, resulting in large non-dimensional roll rate values in an uncoordinated condition. The residual body axis terms in the Kalviste decomposition reveal the nature of the uncoordinated motion (figure 4C). As pointed out in the in-control discussion, the magnitude of these terms is significant enough to encompass a large range of non-linear damping behavior, and as shown in figure 4a, the peak body axis roll rate is nearly coincident with the peak sideslip value. The amplitude of the roll motion (roll angle in figure 4b) also shows that during this uncoordinated excursion, the displacement of ϕ is over 90°. These conditions are pointed out since the typical linearized damping terms that would be used to characterize the departure dynamics are those taken at zero sideslip angle at a single, low, non-dimensional rate, with typically a +5° to -5° roll oscillation amplitude. Obviously, any effects of rate, sideslip, or amplitude on the body axis damping terms would impair the conventional test method's ability to accurately model the vehicle's true response

Two examples of the the falling leaf motion were examined, with one shown in figures 5 and 9. Both motions examined were entered at low to slightly negative angle of attack, departing after significant sideslip buildup during an attempted rudder roll. The presented PAX Flight 12.9 departs after intentional cross control input. Regardless of the control input, the application of rudder at low angle of attack cause the two seat canopy, centerline tank equipped configuration to build excessive sideslip. This occurs for this configuration because the available rudder power is sufficient to drive sideslip past the point where it becomes unstable directionally (that extended past the limits of the original database), resulting in very large

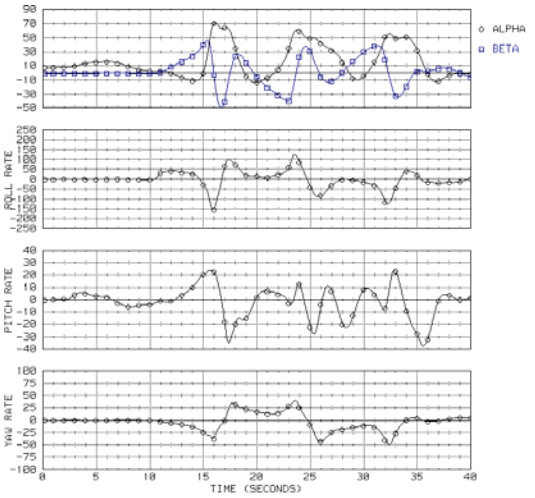

Figure 5a. Falling leaf motion, rates and angles

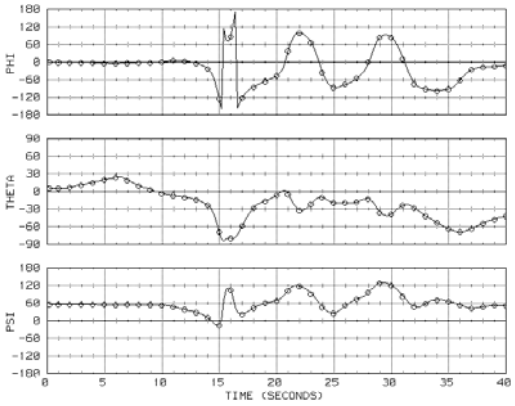

Figure 5b. Falling leaf motion, angles

excursions until the lateral stability (low at low angles of attack) causes the airplane to roll. The kinematic coupling between sideslip and angle of attack then produces the rapid angle of attack buildup, and the ensuing oscillation is a complex interplay of the static and dynamic characteristics. While the non-dimensional roll and yaw rates are substantial, they remain the same sign through the oscillation cycle (the resulting nose up pitching moment that occurs during this condition being one of the motion's forcing functions) the motion does not remain coordinated because of the large angular fluctuations. Consequently, this motion excites both coordinated wind axis oscillations with superimposed uncoordinated body axis motions. As in the case of the departure mentioned earlier, these body axis excitations occur during a range of sideslip, rate, and amplitude conditions that are currently unavailable in the test world. These motions add a further level of potential dependency on the effect of varying combinations of lateral-directional rate excitation ranging from coordinated to fully uncoordinated. As mentioned earlier, the sideslip and rate dependencies are substantial in the rotary data set and are typically modeled, however, none of these functionalities are addressed in the body axis damping data.

The oscillatory, intermediate yaw rate spin presented in figure 6 depicts a less oscillatory case than the falling leaf motion. While the sideslip and roll rate oscillations are substantial, the spin develops a relatively constant yaw rate, producing the heading change that characterizes the motion. Interestingly, the non-dimensional pitch rate oscillation is considerably greater the those seen in the falling leaf, which surprisingly have very low pitch rate oscillations. Because of the relatively coordinated condition that occurs during the spinning motion, the rate excitation tends to be predominately about the velocity vector, however, the oscillatory nature of the spin does excite

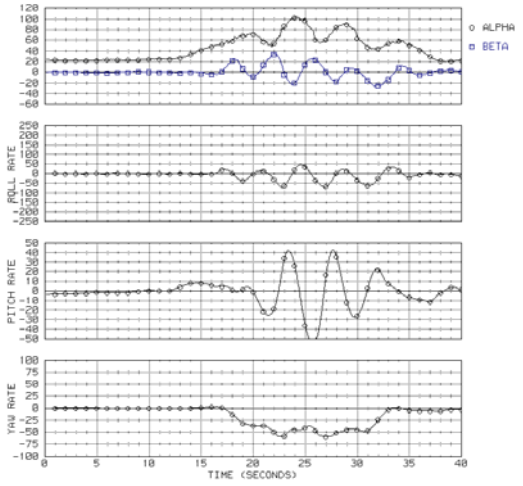

Figure 6. High aoa spin motion, rates and angles

substantial body axis roll rates as well. (It should be pointed out that as the spin approaches a smooth condition, the relevance of the body axis damping terms is greatly reduced relative to the velocity vector damping). More so than the falling leaf motion, these body axis rates are essentially superimposed over the velocity vector rates. Like the falling leaf, all the body axis rates, including pitch, are excited in the presence of large sideslip variations.

Summarizing the observations of the flight test motions versus the database requirements reveals several conclusions. The most prominent, and intuitive, is the importance of the first order terms: the static database and the characterization of all important functionalities. This includes the effect of sideslip on the basic airframe as well as on all controls, and ensuring that the sideslip modeling is sufficiently extensive to encompass out-of-control excursions. When analyzing the in-control motions, the damping effects are most important in the wind axis system, as defined by the rotary derivatives. During departures, uncoordinated body axis rates are prevalent and the need for accurate quantification of these effects is paramount. Because of the range of rates experienced and the likelihood of non-linear variation in the stall/post stall region, quantification of these effects may be needed as part of high fidelity non-linear modeling. Since the development of uncoordinated rates typically is coincidental with sideslip excursions during departure, the potential variation of damping with these functionalities may warrant the inclusion of these effects. Fully departed motions are frequently characterized as combinations of coordinated and uncoordinated motions. The impact of superposition of these terms is currently unresolved as a testing issue and will be addressed from a data mechanization stand

point in subsequent discussion. The underlying inference for both the static and dynamic terms is the need to collect test data that encompasses the anticipated excursions of the modeled vehicle, as well as identifying and modeling the appropriate functionalities for each term. Analysis efforts involving the development of test techniques as well as evaluation of modeling requirements are needed to address the database level of detail required in order to accurately simulate these motions. This effort would hopefully restrict the required test matrix to a reasonable size.

Effect Of Mechanization

Evaluation of the effects of mechanization focuses on several of the flights presented earlier: HARV flight 172.11, PAX flight 11, and PAX 12-9. All the coefficient comparisons discussed in the following section were generated using the 'overdrive' technique discussed earlier.

The velocity vector roll maneuver (figures 3 and 7) shows how the flight extracted rolling moment changes direction from roughly neutral to opposing the direction of roll, as the roll rate is arrested (figure 7a). As shown in the figures, if the dynamic derivatives are used exclusively for the damping (no rotary), the propagated rolling moment remains in the direction of the roll rate throughout the maneuver. The component breakdown of the dynamic rolling moment increment shows that the sum of the dynamic increment due to roll rate and yaw rate is the source of the large pro-roll rate rolling moment increment, specifically, the yaw rate damping effect (figure 7b). This example shows how the combination of the two linearized forced oscillation terms is inadequate to model the rolling moment for a coordinated maneuver at elevated angle of attack. When the rotary damping terms (whose test motion matches the actual flight test vehicle's motions) are utilized to describe the damping through either the direct or Kalviste implementation methods, the correlation between the simulation and flight data is considerably improved during the roll portion of the maneuver. This is due to the rotational roll damping, as shown in the dynamic rolling moment term buildup in figure 7b, which is much less damped than the previously shown mechanization. The yawing moment terms, as presented in figures 7a and 7c, show that the dynamic yaw damping totals result in a very similar increment regardless of the data mechanization scheme used. Because of the large yaw increment that results from the use of thrust vectoring in yaw during this maneuver (also included in the total yaw coefficient), any further resolution in the yaw axis was obscured.

The next maneuver evaluated was a departure following a roll reversal at elevated angle of attack. As shown in figures 4 and 8, this departure occurs at

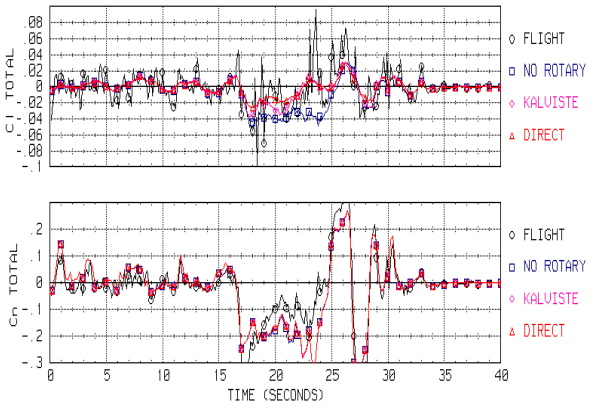

Figure 7a. Velocity vector roll, Cl and Cn components

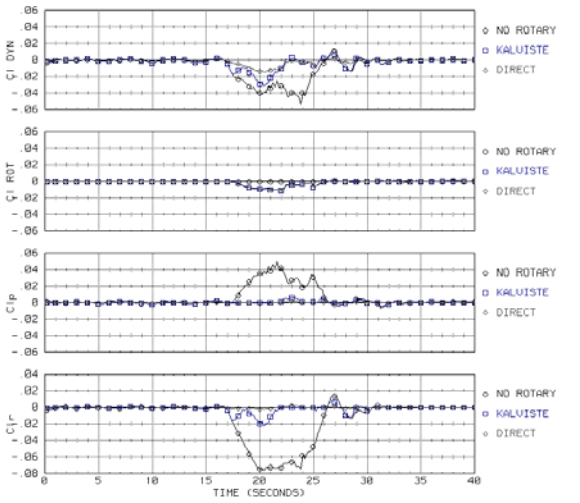

Figure 7b. Velocity vector roll, Cl components

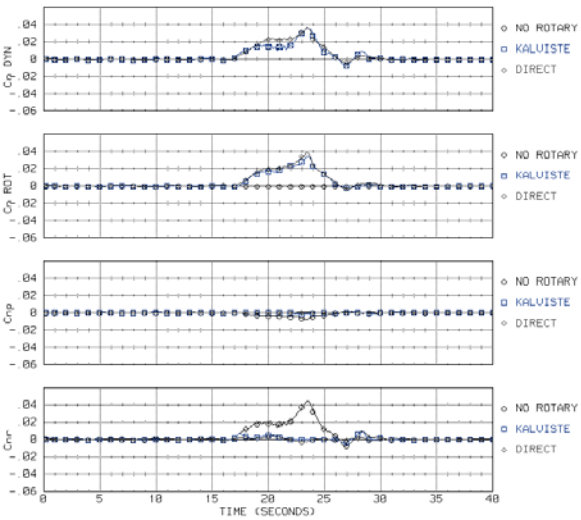

Figure 7c. Velocity vector roll, Cn components

approximately 30° angle of attack as the vehicle attempts to reverse the roll angle and a large sideslip, resulting in a large uncoordinated roll rate. When using only forced oscillation data to describe the dynamic damping in this case, the correlation with flight test is degraded in both roll and yaw (figure 8a). When the rotary data is introduced, the rolling moment match with flight test is relatively unchanged, while the correlation in yaw is improved during the peak rate excitations. Examination of the components of the lateral-directional dynamic terms reveals the reasons for these results. The components in roll, when the forced oscillation data are used exclusively, are presented in figure 8b. Note how the large values of the dynamic terms Clp and Clr at these angles of attack result in very high peak moment values. Even though the damping due to the yaw rate term opposes the damping due to roll rate, because of the magnitude of the roll rate term, the resulting total damping is still large and is responsible for the discrepancy with the flight extracted model. When the rotary terms are introduced, the total roll increment due to body axis roll rate is reduced, but does remain substantial, as the over coordinated nature of the motion resolves the rates between rotary damping and the body axis roll damping using Kalviste's method. As a result, the effect of the rotational damping (slightly undamped in this case) is diminished by the size of the body axis contribution. When evaluated against the flight data, it is clear that the large body axis roll damping contribution accounts for the poor correlation with flight during the period of roll rate excitation. Inspection indicates that a substantially reduced body axis rate damping term (near zero) would significantly improve correlation with flight. These results are consistent with flight extraction results obtained independently at these angles of attack (e.g. figure 1, reference 7). The fact that the body axis terms resist the rate development significantly impacts the modeling and evaluation of departure characteristics and points to the need to re-evaluate the dynamic test data in this region. The dynamic yawing moment terms obtained with the Kalviste implementation are shown in figure 8a, where the rotary data imposes a damping increment, with little contribution from the body axis terms. Because of this damping effect, the correlation of the yawing moment with flight is improved using this mechanization.

The effect of the modeling implementation during an out of control 'falling leaf' motion was also examined, and is presented in figures 5 and 9. Following rudder application at approximately -5° angle of attack, a large sideslip excursion occurs with a subsequent departure into a repetitive out of control motion that exhibits large rate and angular excursions. Because of the large angular displacements that occur,

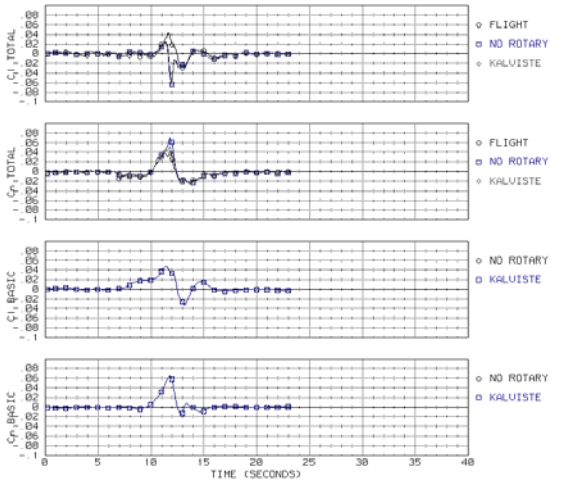

Figure 8a. Departure at 30° aoa, Cl and Cn components

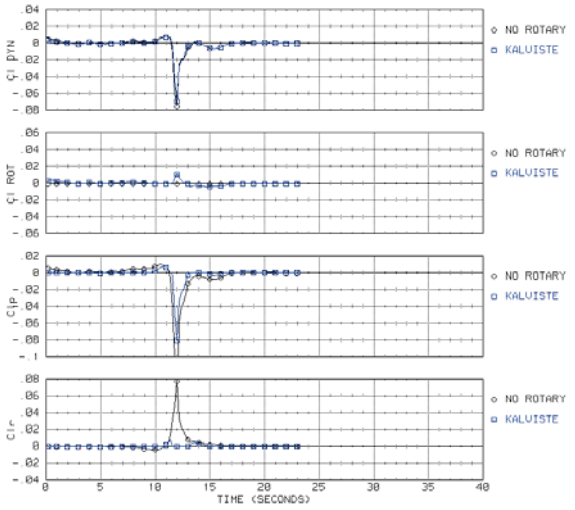

Figure 8b. Departure at 30° aoa, Cl components

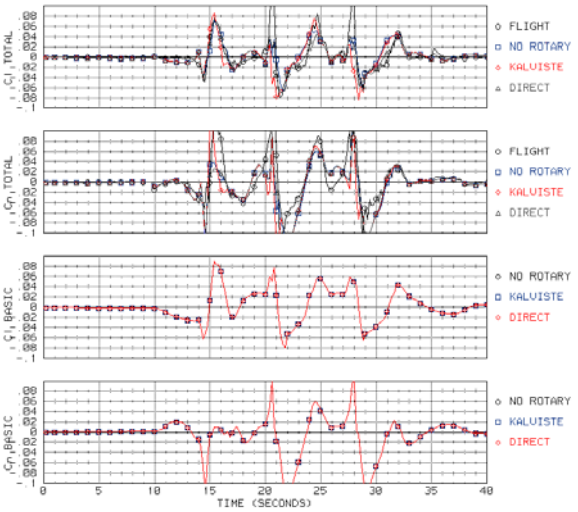

Figure 9a. Falling leaf motion, Cl and Cn components

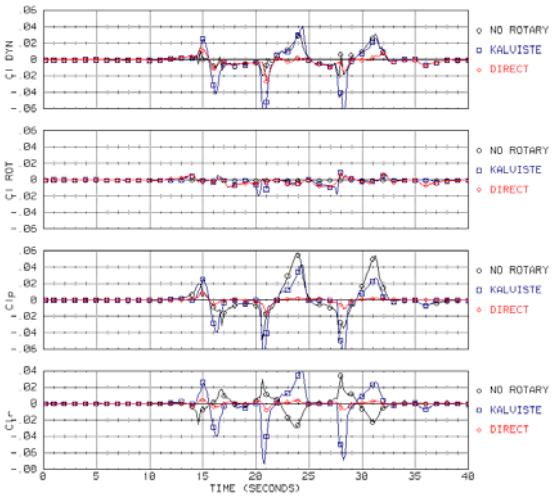

Figure 9b. Falling leaf motion, Cl components

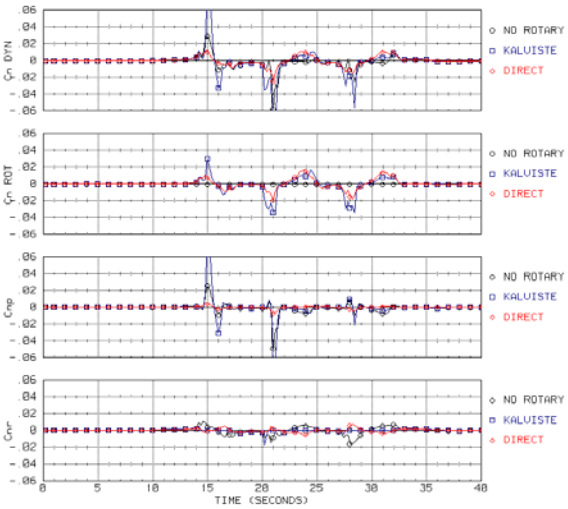

Figure 9c. Falling leaf motion, Cn components

the static effects predominate the coefficient propagation during the maneuver (figure 9a, see C_{lBasic} and C_{nBasic}). As a result, the ability to resolve the differences due to the dynamic contributions in a comparison of roll and yaw contributions is diminished. A comparison of the effect of using various mechanizations (such as to rotary balance data, direct resolution on the velocity vector, filtered wind axis, and the Kalviste method) on the dynamic roll and yaw terms are shown in figures 9b and 9c, respectively. Various dynamic components for each of these mechanization techniques are presented. These plots reveal a number of differences that differentiate the various mechanization schemes. By exclusively using the forced oscillation data, the dynamic roll increment is the sum of two large body axis terms whose sum is similar to the dynamic roll increment obtained when using the Kalviste method. Similar results in the yaw axis (figure 9c) reveal the characteristics that differentiate the Kalviste method from resolving purely about the velocity vector (direct method). The uncoordinated motion that occurs during the maneuver permits the excitation of the body axis terms when Kalviste's method is used. Using either the direct or the filtered wind axis method both result in little excitation in the body axis, however, with substantially different roll and yaw propagation. As described earlier, the differentiation of these mechanization schemes when compared to the flight propagated coefficients are somewhat obscured by the substantial static effects.

CONCLUSIONS

The NAWC/AD Manned Flight Simulation Center F/A-18 simulation has been used as an evaluation tool to examine the requirements of the simulation database versus selected in-control and out-of-control flight regimes. In addition, the effect of dynamic data implementation schemes on the simulation response was also evaluated. Analysis of the flight data reveals that many of the motions exceed the database coverage of even a large, non-linear database such as the F/A-18's; i.e., sideslip excursions during departures can exceed 50°, influencing the basic airframe, controls and dynamic terms. The need to characterize all the static data as a function of this non-linear dependency is clear. Further analysis of the dynamic damping indicates the effect of sideslip, and particularly, the effect of rate needs to be investigated as a potential functionality. While these dependencies are typically incorporated in most wind axis damping test data (rotary balance data), little investigation of these effects on the body axis damping terms has ever been conducted. For example, most existing body axis damping data is collected at nondimensional rates well below those experienced in departures, and as a derivative, the higher rate effects are extrapolated.

As part of the analysis of the dynamic data mechanization, the existing database was updated, where possible, with available test data to correspond with conclusions described above. One of the most significant changes was the inclusion of the original body axis damping wind tunnel test data. With these changes, the evaluation of the dynamic data mechanization schemes showed how the inclusion of the rotary data, through the use of a mechanization such as that proposed by Kalviste, can improve the fidelity of the simulation. This is particularly evident when evaluating coordinated maneuvers near or beyond stall. The body axis damping terms become significant during uncoordinated flight conditions, such as departures, and their magnitude can significantly influence the simulated results. However, there remains

evidence, for the same reasons discussed above, that these test data are not currently representative of the conditions the airplane experiences in these motions.

Finally, the updated simulation, along with the recommended mechanization technique, was validated for normal flight regime maneuvering using simulation validation flight test data. These results supported the observations detailed in the analysis of the higher angle of attack regime; where applicable, the data and mechanization changes effects' ranged from a general improvement to little or no change in the simulation's fidelity during lower angle of attack maneuvers.

ACKNOWLEDGMENTS

The authors express their gratitude to Bill McNamara, Chad Miller, Mike Bonner, and Mike Brunner at NAWC/AD Manned Flight Simulation Facility for their assistance in providing simulation environment maintenance, operation, and time histories of numerous F/A-18 C/D flight maneuvers. Thanks also to Joe Wilson at NASA Dryden for providing time histories of F/A-18 HARV flight maneuvers.

REFERENCES

1. Ralston, J. N. and Avent, J. L.: Evaluation and Modification of F/A-18B Aerodynamic Database for Improved Departure Modeling, BAR 92-2, March 1992.
2. Kalviste, Juri: Use of Rotary Balance And Forced Oscillation Test Data In A Six Degrees Of Freedom Simulation, AIAA Paper 82-1364, Aug. 1982.
3. Hess, Robert A.: Simulation Checking Using An Optimal Prediction Evaluation (SCOPE) User Guide, SCT 4522-270-2, September, 1987.
4. Ralston, J.: Analysis of F-18A/B Low Speed, High Angle of Attack Aerodynamic Database, BAR 88-7 September, 1988.
5. O'Connor, C.: NATC F-18A/B Aerodynamic Math Model Modifications Incorporated During the Phase I Model Unification Effort, BAR 89-5, March, 1989.
6. O'Connor, C.: NATC F-18A/B Aerodynamic Math Model Modifications Incorporated During the Phase II Model Unification Effort, BAR 90-13, Sept. 1990.
7. Hess, R. A.: Subsonic F/A-18A and F/A-18B Aerodynamics Identified from Flight Test Data, SCT-4522-220-1, July, 1987.
8. Hess, R. A.: Effect of Various Stores on the Aerodynamics of an F/A-18B Aircraft Identified from Flight Test Data, SCT-6612-020-2, February 1989.
9. Bihrle, W., Jr.; and Barnhart, B.: Spin Prediction Techniques. Journal of Aircraft, vol. 20, no. 2, Feb. 1983, pp. 97-101.
10. Grafton, S., et al.: High Angle-Of-Attack Stability Characteristics Of A Three-Surface Fighter Configuration, NASA TM 84584, March 1983.
11. Tobak, M. and Schiff, L.: On The Formulation Of The Aerodynamic Characteristics In Aircraft Dynamics, NASA TR R-456, January 1976.
12. Beyers, M.: A New Look At The Tobak-Schiff Model Of Nonplanar Aircraft Dynamics, NAE-LTR-UA-101, Ottawa, Canada, December 1989.
13. Penna, P. and Beyers, M.: Support Interference Assessment In Rotary Experiments Using The Orbital Platform Concept, IAR-AN-79, Ottawa, Canada, April 1994.
14. Ericsson, L. and Reding, J.: Dynamic Support Interference In High-Alpha Testing, Journal Of Aircraft, Vol. 23, No. 12, December 1986.
15. Fitzgerald, T., Ralston, J. and Hildreth, B.: Improvements To The Naval Air Warfare Center Aircraft Division's F/A-18 Subsonic Aerodynamic Model, AIAA94-3400, August 1994.
16. Anon, F15E High Angle of Attack Wind Tunnel Test Program - Final Technical Coordination Meeting Presentation, March 1994.
17. Shows, MAJ R.J., Mumfrey, MS. G. D., Evaluation of the FA-18B Airplane Departure Resistance and High Angle of Attack Flying Qualities, NATC Report: SA-141R-86.
18. Ralston, J., Dickes, E., Application of Dynamic Data in Aircraft Simulation, BAR 95-1, Jan. 1995.
19. Jaramillo, P., and Ralston, J.: Simulation and Analysis of the F/A-18D Falling Leaf Motion with an Assessment of Suppression Strategies, Bar 95-8, Dec. 1995.
20. Jaramillo, P., and Ralston, J.: Simulation of the F/A-18D Falling Leaf, AIAA96-3371.
21. Jaramillo, P.: An Analysis of Falling Leaf Suppression Strategies for the F/A-18D, AIAA96-3370.
22. Ralston, J., and O'Connor, C.: Evaluation Of The NAWC/AD F/A-18 C/D Simulation Including Database Coverage And Dynamic Data Implementation Techniques, BAR 95-3, December 1995.